Food Chemistry: X 26 (2025) 102295

Contents lists available at ScienceDirect

Food Chemistry: X

journal homepage: www.sciencedirect.com/journal/food-chemistry-x

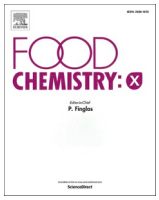

# Lipid oxidation and lipidomic profiles of raw and thermal-extracted yak fat under hydroxyl radical-induced oxidative stress

Sining Li [a], Shanhu Tang [a,*], Ran Mo [a], Pinglian Yu [b]

[a] College of Pharmacy and Food, Southwest Minzu University, Chengdu 610041, China
[b] School of Chemistry and Chemical Engineering, Zhaotong University, Zhaotong 657000, China

ARTICLE INFO

*Keywords:*
Lipid oxidation
Lipidomics
Hydroxyl radical
Thermal extraction
Yak fat

ABSTRACT

The lipid profiles in raw fat (RF) and thermal-extracted fat (TF) from yak under hydroxyl radical-induced oxidative stress were investigated. Both hydroxyl radical and thermal extraction accelerated lipid oxidation. A total of 1168 lipids were identified and classified into 18 lipid categories. The top eight classes of lipids included PCs, PEs, TGs, SMs, CERs, PSs, FAs and PAs. Furtherly, 432 differentially abundant lipids were detected in TF samples compared to RF samples. RF and TF samples displayed a complete distinction in lipidomic profiles, and some lipids in both RF and TF samples demonstrated remarkable differences in abundance with the increasing of $H_2O_2$ concentration. RF samples demonstrated a relatively higher abundance of PCs, PEs, PSs, PGs and PIs, while TF samples exhibited a higher level of PAs, TGs, FAs and CERs. These findings indicated that radical attack and thermal extraction severely affected lipid oxidation and lipid metabolomics.

## 1. Introduction

Animal fat plays a crucial role in the development of nutritional and sensory characteristics in meat and meat products, which is attributed to the fact that lipids in meat act as the main source of energy and major precursors of meat flavor (Shin et al., 2019; Song et al., 2011). However, lipids are susceptible to oxidation with the presence of several initiators during processing and storage of meat products, such as heating, lighting, free radical and metal catalyst, resulting in the generation of rancidity and off-flavor, changes of color, formation of toxic compounds, and loss of nutritive value to a certain extent (Tu et al., 2022). Currently, lipid oxidation has been considered as a main factor that has negative impact on the quality of meat and meat products (Abeyrathne et al., 2021; Amaral et al., 2018).

Lipid oxidation occurs and develops mainly via a chain reaction of free radical-mediated, especially under the condition of reactive oxygen species (ROS), reactive nitrogen species (RNS), and/or some secondary oxidation products present in muscle food matrices (Amaral et al., 2018; Tu et al., 2022). The radical reaction consists of three stages: initiation, propagation, and termination (Kanner, 1994). The primary lipid oxidation products like hydroperoxides, have little effect on the meat quality (e.g., odor and flavor), whereas the secondary products derived from the decomposition of hydroperoxides, some of which are volatiles with very low odor thresholds, critically affect the organoleptic properties of the matrices (Song et al., 2011). In addition, the secondary oxidation products, such as malondialdehyde, are capable to modify proteins, phospholipids and so on, potentially altering their structure and function (Beavers et al., 2014). There are numerous studies on lipid oxidation in muscle foods reporting that the overall quality could be estimated by classical chemical parameters, such as peroxide value, acid value, free fatty acids, and thiobarbituric acids (Coombs et al., 2018; Abeyrathne et al.,2021). Nevertheless, due to the highly unstable intermediate products produced during the oxidation process, the traditional assays for the lipid oxidation mentioned previously only provide limited information about oxidation damage (Tu et al., 2022). Therefore, it is of great significance to reveal the characteristics of lipid oxidation at the molecular level.

Lipidomics served as a novel comprehensive approach, is employed to accurately and thoroughly describe the lipid species, thus provides more detailed coverage of lipid compositions and metabolites (Li et al., 2021). In recent years, lipidomics based on mass spectrometry has been successfully used for monitoring the alternations in substrates and products of lipid oxidation (Bao & Pignitter, 2023; Tu et al., 2022). Previous publications confirmed the effectiveness and reliability of liquid chromatography-mass spectrometry (LC-MS) lipidomics to determine lipid oxidation markers, which provided a deep and extensive

* Corresponding author.
*E-mail address:* stang01@126.com (S. Tang).

https://doi.org/10.1016/j.fochx.2025.102295
Received 2 December 2024; Received in revised form 25 January 2025; Accepted 16 February 2025
Available online 19 February 2025

understanding of the lipid profile changes in muscle food triggered by hydroxyl radical (Tu et al., 2022; Wang et al., 2024; Zhu et al., 2024).

Yak fat was reported containing several functional fatty acids, such as omega-3 fatty acids commonly including eicosapentaenoic acid (EPA) and docosahexaenoic acid (DHA). These fatty acids play important roles in the human nutrition. It has been reported that the yak subcutaneous fat contains relative high content of unsaturated fatty acids (Xiong et al., 2022), which implies that the lipids in yak fat are prone to be oxidized during processing and storage. Generally, rendering is used to improve the edible quality and oxidative stability of the fat (Wojtasik-Kalinowska et al., 2021). This rendering or thermal extraction process can inactivate enzymes, and remove moisture and impurities from the raw fat that affect the storage stability of fat. However, the lipids oxidation in adipose tissue is accelerated via the attack of free radicals during rendering and resulting in numerous products with different structures. Therefore, it is necessary to study the relationship between the attack of free radicals on target lipids and their products.

To the best of our knowledge, few information has been published focusing on the differences in lipid profiles of the raw fat and thermal-extracted fat based on lipidomic technique. In this scenario, the objective of this study was to characterize the lipidomic profiles of raw or thermal-extracted yak fat exposed to the most commonly free-radical generating system using a LC-MS/MS lipidomic approach. This study could be conducive to understand the molecular mechanism of lipid oxidation in yak fat, and to provide a fundamental basis for explaining the development of lipid profiles during thermal-extraction and oxidation. The result provides theoretical guidance for reducing the oxidative damage during oils and fats processing.

## 2. Material and methods

### 2.1. Chemical reagents

Reagents of ethylene diamine tetraacetic acid (EDTA), gallic acid, 2-thiobarbituric acid (TBA), 2,6-di-tert-butyl-4-methylphenol (BHT), and tetraethoxypropane were obtained from Shanghai Yuanye Bio-Technology Co., Ltd. (Shanghai, China). Reagents for LC-MS analysis including acetonitrile, isopropanol, and methanol were of LC-MS grade and were obtained from Thermo Fisher Scientific (Waltham, MA, USA). Formic acid, ammonium acetate, and methyl tertiary butyl ether (MTBE) were purchased from Thermo Fisher Scientific (Waltham, MA, USA). The remaining chemicals with a minimum analytical grade were acquired from Chengdu Kelong Chemical Co., Ltd. (Chengdu, China).

### 2.2. Raw and thermal-extracted yak fat

Four healthy adult male Maiwa yaks (3 to 4 years old) weighing approximately of 190 kg under the same natural grazing condition were selected randomly from a pasture in Hongyuan County, Sichuan Province, China. After 24 h of water deprivation and stunned by electric shock, yaks were slaughtered humanely following the Operating Procedures of Cattle Slaughter - the National criterion of P.R. China (China, 2018) in a commercial abattoir (New Hope Yak Industry Co. Ltd., Hongyuan, Sichuan) and the raw subcutaneous fat samples were collected from the postmortem carcasses and delivered to our laboratory by a refrigeration container. The thermal extraction process of yak fat was followed a previously described beef tallow extraction method with slight modifications (Nam, 2022). The raw yak fat samples were sliced as 1 cm cubic pieces, and then were heated with a temperature of 115 °C for 2 h in a steel-stainless container. Followingly, the residues and the insoluble impurities were removed from the extracts by four layers of cheese cloth. Finally, the yak fat was cooled to room temperature (20 ± 2 °C) until solidified.

### 2.3. Oxidation system

Phosphate buffer solution with a concentration of 0.02 mol/L (pH 6.0) for hydroxy radical generation was prepared according to the method stated by Cao et al. (2020), which contained 0.01 mmol/L of $FeCl_3$, 0.1 mmol/L of ascorbic acid, and various concentrations of $H_2O_2$ (0, 10, 20 or 30 mmol/L). The raw fat (RF) samples or thermal-extracted fat (TF) samples were prepared as 1 cm cubic size. Next, the prepared RF samples randomly assigned to 4 treatments by 3 times, and the corresponding samples were mixed in a ratio of 1:4 (*w/v*) with the buffer containing 0, 10, 20, or 30 mmol/L $H_2O_2$. The TF samples were treated in the same way as the RF samples. All the samples were subjected to oxidations at 4 °C for 24 h, after which the reactions were instantly terminated by adding 1 mmol/L of EDTA. The liquid was discharged and the residual fats were washed two times with phosphate buffer (0.02 mol/L, pH 6.0) to remove the oxidant. Then the fat samples were immediately analyzed for lipid oxidation and lipidomic properties.

### 2.4. Peroxide value determination

The peroxides were determined as described by Shantha and Decker (1994). Approximately 2 g of prepared fat samples were homogenized, at 12,000 rpm for 30 s, with 15 mL mixed solution of chloroform-methanol (2:1, *v/v*) containing 0.05 % (*w/v*) of antioxidant BHT. Then, a volume of 3 mL 0.5 % (*w/v*) NaCl was incorporated, vortexed rapidly for 15 s, and centrifuged at 4 °C at 3000 ×*g* for 10 min. A portion of 5 mL from the bottom phase was collected and blended well with equal volume of the mixed solution of chloroform-methanol (2:1, *v/v*), and 25 μL of 30 % (*w/v*) ammonium thiocyanate. Subsequently, 25 μL of $FeCl_2$ solution was pipetted into the tube and mixed up, and the system was immediately incubated for 20 min under a temperature of 20 ± 2 °C. Finally, the absorbance of the solution was determined with a spectrometer at wavelength of 500 nm. Pure iron powder was used for preparation of standard curve and the blank was designed to contain all the reagents except for the fat sample. The peroxide value was calculated by the equation:

$$\text{Peroxide value (meq/kg)} = \frac{k \times (A_s - A_b)}{55.84 \times m \times 2} \times 1000$$

where $k$ is the slope of the curve, $A_s$ is the absorbance of the fat sample, $A_b$ is the absorbance of the blank, 55.84 is the atomic weight of iron, $m$ is the mass of the sample (g), 2 is the division factor.

### 2.5. Acid value determination

The acid value was evaluated by a standard titrimetry method reported by Shin et al. (2019). A portion of 5 g fat sample was mixed well with 20 mL of ethyl ether-ethanol (2:1, *v/v*) and incubated in the dark for 60 min at 20 ± 2 °C. Then, 2–3 drops of 1 % (*w/v*) phenolphthalein as indicator was added and immediately titrated with 0.1 mol/L KOH to the end point of light red color. Acid value was calculated by the equation:

$$\text{Aacid value (mg KOH/g)} = \frac{v \times c \times 56.11}{m}$$

where $v$ represents the volume number (mL) of consumed KOH, $c$ denotes the concentration of KOH in normality, $m$ is the fat sample weight (g).

### 2.6. Thiobarbituric acid reactive substances (TBARs) determination

TBARs value was assessed by following the procedure delineated by Jongberg et al. (2011) with slight modifications. A portion of 10 g fat sample was mixed with 30 mL of 7.5 % (*w/v*) trichloroacetic acid solution containing 0.1 % (*w/v*) gallic acid and 0.1 % (*w/v*) EDTA. Then,

the mixture was homogenized for 60 s using a homogenizer (IKA, Baden-Württenberg, Germany) with a speed of 12,000 rpm. After filtration, a volume of 7 mL of the filtrate was mixed up with 5 mL of 20 mmol/L TBA and instantly incubated in boiling water for 40 min. After cooling down, the absorbance of the filtrate was read at wavelengths of 532 and 600 nm. TBARs value was quantified by a calibration curve plotted with absorbance by a solution of tetraethoxypropane (Serra et al., 2014), and expressed as mg of malondialdehyde (MDA) per kg of fat sample.

### 2.7. Lipidomic analysis

#### 2.7.1. Sample extraction

The extracts were obtained according to the procedure stated by Jia et al. (2021) with minor modifications. In brief, 100 mg of fat samples and 0.75 mL of ice-cold methanol were pipetted into a glass tube and completely mixed by vortexing for 60 s, and then a volume of 2.5 mL cold MTBE was added and incubated in a compartment at 20 ± 2 °C for 1 h. Followingly, a volume of 0.625 mL water (LC-MS grade) was pipetted into the tube and the sample was centrifuged at 3000 ×*g* for 10 min (4 °C) to separate the organic and inorganic phase. The upper layer was collected and the lower layer phase was washed with 1 mL of MTBE/methanol/water (10:3:2.5, *v/v/v*) following the same procedure. The supernatants from both the extraction step were combined and dried with nitrogen stream. The dried product was resuspended in 100 μL of isopropanol and then traversed through a 0.22-μm microporous membrane for further analysis.

#### 2.7.2. UPLC-MS/MS analysis

Lipidomic analysis was conducted using a Vanquish UPLC system (Thermo Fisher Scientific, Germany) with an Accucore $C_{30}$ column (2.1 × 150 mm, 2.6 μm, Thermo Fisher Scientific, Germany) coupled to an Orbitrap Q Exactive™ HF mass spectrometer (Thermo Fisher Scientific, Germany). The chromatographic column temperature and the flow rate was 40 °C and 0.35 mL/min, respectively. A volume of 5-μL sample was injected. The eluted mobile phase A was mixed solution of acetonitrile/water (60:40, *v/v*) containing 10 mmol/L of ammonium acetate and 0.1 % (*w/v*) formic acid, whereas eluted mobile phase B was mixed solution of isopropanol/acetonitrile (90:10, *v/v*) containing 10 mmol/L ammonium acetate and 0.1 % (*w/v*) formic acid. The elution gradient was programmed for 20 min as follows: 0–2 min, 30 % mobile phase B; 2–5 min, 30–43 % mobile phase B; 5.1–11 min, 55–70 % mobile phase B; 11–16 min, 70–99 % mobile phase B; 16–18 min, 99 % mobile phase B; and 18.1–20 min, 30 % mobile phase B.

The mass spectrometer was run in both positive electrospray ionization ($ESI^+$) and negative electrospray ionization ($ESI^-$) and alternated between full scan (114–1700 *m/z*). The parameter settings including sheath gas (20 psi), sweep gas (1 L/min), auxiliary gas rate for $ESI^+$ mode (5 L/min) and for $ESI^-$ mode (7 L/min), spray voltage (3 kV), capillary temperature (350 °C), auxiliary gas heater temperature (400 °C), isolation width for MS/MS (1 *m/z*), and normalized collision energies for $ESI^+$ mode (25 eV and 30 eV) and for $ESI^-$ mode (20 eV, 24 eV and 28 eV) were designed. Quality control (QC) samples and technical replicates were employed for monitoring the intra-batch instrumental drift and batch effects. The QC samples were mixed equally from extracts of each sample.

Data of retention time, mass to charge ratio and ion intensity derived from UPLC-MS/MS were analyzed with the software package of Compound Discoverer 3.1 (CD 3.1, Thermo Fisher Scientific, Germany). Peaks were collected by considering 0.2 min for retention time tolerance, 5 ppm for actual mass tolerance, 3:1 for signal-to-noise ratio, 100,000 for minimum intensity, and 30 % for intensity threshold. The molecular formulas were predicted by using the normalized data derived from additive ions, molecular ion peaks and fragment ions, and the accurate qualitative and relative quantitative results were obtained by matching the peaks with the databases of LIPIDMAPS and LIPIDVLAST.

### 2.8. Statistical analysis

All the experiments were conducted in triplicate, unless otherwise specified. Data were processed using the General Linear Models procedure of SPSS 21.0 (IBM, Chicago, USA), and analyzed with mixed models, in which $H_2O_2$ concentration, fat type and their interaction were fitted as fixed effects, and replicates were fitted as random effects. The results were expressed as mean ± standard error. The significant differences of main effects were identified using Duncan's test for multiple comparisons with a confidence level of 95 %.

Data derived from the mass spectrometric measurements were processed and transformed by metaX software, and R software (v3.4.3) was employed for statistical analyses. Statistically significant difference ($P < 0.05$) was determined by univariate analysis (*t*-test). The overall difference among treatments was evaluated by principal component analysis (PCA). Differentially abundant lipids (DALs) were selected by considering the *P*-value ($P < 0.05$), fold change (FC ≤0.5 or ≥ 2) and variable importance in projection (VIP >1).

## 3. Results and discussion

### 3.1. Peroxide content

Peroxide value is typical and key indicator for assessing the primary products of fat oxidation, which mainly depends on the ratio of formation to degradation of hydroperoxides (Maqsood et al., 2015). As presented in Fig. 1A, $H_2O_2$ concentration, fat type and their interaction had remarkable effects on the peroxide value ($P < 0.05$). The RF samples had the highest peroxide value (0.24 meq/kg) when 20 mmol/L $H_2O_2$ was added, although there was no observable difference between 10 mmol/L and 20 mmol/L, while the peroxide value of TF samples elevated to a peak (0.35 meq/kg) at 10 mmol/L $H_2O_2$. The decline in peroxide value was probably ascribed to the fact that unstable lipid hydroperoxides were decomposed to multiple secondary oxidation species, such as small molecules of aldehydes, ketones, alcohols and short-chain hydrocarbons, at a faster rate than new hydroperoxides were formed (Zhang et al., 2020). Notably, thermal extraction was found to significantly increase the formation of lipid peroxides in TF samples, and the effect for improving peroxides was also reported by Abdulkadir and Jimoh (2013) by comparative analysis of extracted and fresh tallow. This can most likely be ascribed to the event that the thermal treatment during extraction as one of initiators for the lipid oxidation, resulted in facilitating the mixing of lipids and oxidative catalysts (Zeb & Akbar, 2018).

### 3.2. Acid value

The acid value is derived from the hydrolysis and oxidation of triacylglycerol (TG), mainly quantitively reflecting the free fatty acids (FFAs) in the lipid fraction (Amaral et al., 2018). The changes in acid value of RF and TF samples upon oxidative stress are plotted in Fig. 1B. Results showed that $H_2O_2$ treatment and fat type had significant effects on the acid value ($P < 0.05$), but their interaction did not notably affect the acid value ($P > 0.05$). The acid value of both treatments showed a raising trend ($P < 0.05$) as the $H_2O_2$ concentration increased from 0 to 30 mmol/L. The gradual increase of the acid value may be considered the accumulation of chemical components derived from the degradation of primary products of lipid oxidation (Boran et al., 2006). In general, the increased acid value in muscle food might be associated with development of undesirable sensory quality and textural attributes in meat and meat products (Zhang et al., 2020). As shown in Fig. 1B, the acid value of the RF samples was lower than that of the TF samples regardless of $H_2O_2$ concentration. These observations suggested that thermal extraction accelerated lipid oxidation and hydrolysis in yak fat. Compared to the samples without $H_2O_2$, the acid value of RF and TF soaking in 30 mmol/L $H_2O_2$ increased by 42.62 % and 21.96 %, respectively. It indicated that the lipids in RF samples was more

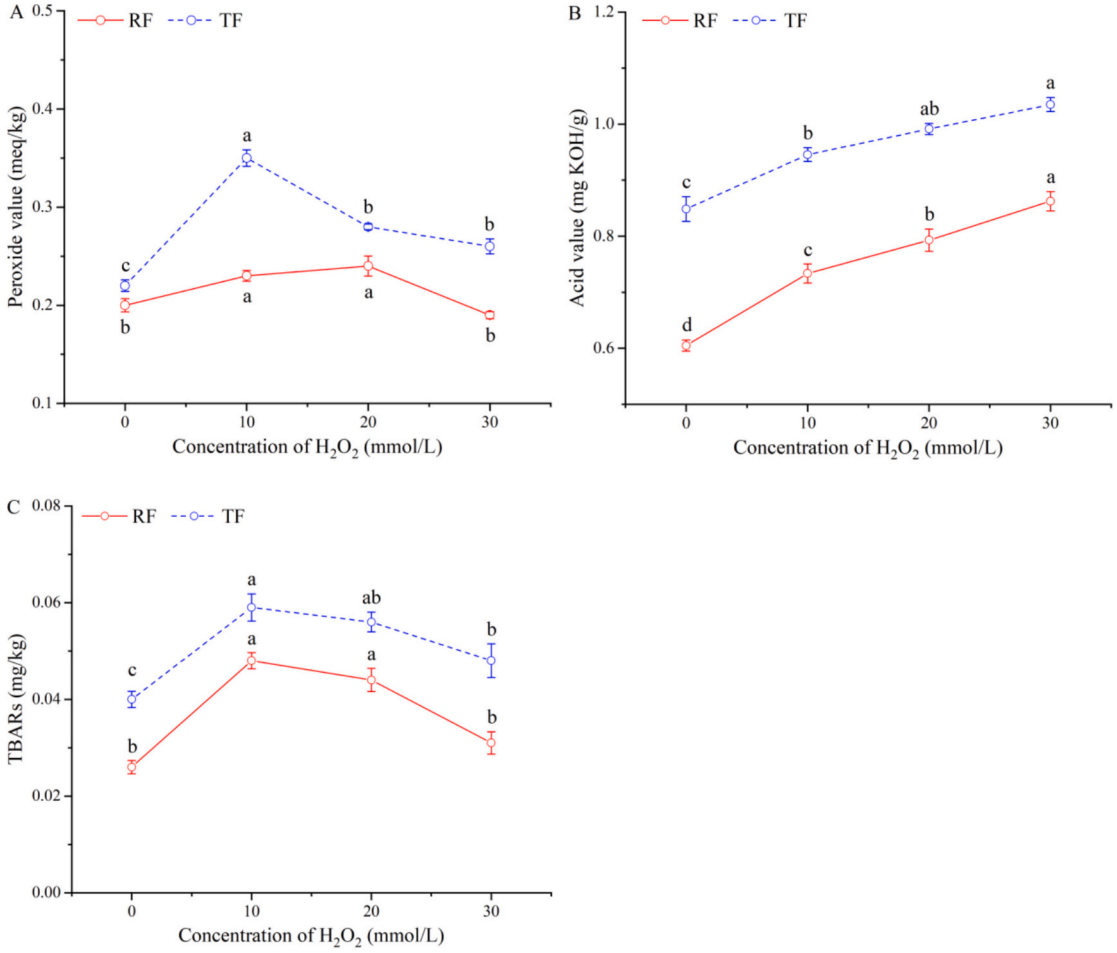


**Fig. 1.** Changes in peroxide value (A), fatty acid value (B) and TBARs content (C) of raw fat (RF) samples and thermal-extracted fat (TF) samples upon oxidative stress. Error bars represent the standard error. [a-c]Means with different lowercase letters are significantly different among $H_2O_2$ treatments ($P < 0.05$).

susceptible to the oxidation than that in TF samples.

### 3.3. TBARs content

The TBARs content is closely related to the number of secondary products of lipid oxidation, such as MDA (Amaral et al., 2018; Maqsood et al., 2015). Fig. 1C shows the evolution of TBARs in samples treated with hydroxyl radicals. Similar with acid value, $H_2O_2$ dosage and fat type significantly affected the TBARs content ($P < 0.05$), but their interaction had no obvious effect on the TBARs value ($P > 0.05$).The TBARs content for both RF and TF increased ($P < 0.05$) as the addition of $H_2O_2$ elevated to 10 mmol/L, and remained steady between 10 and 20 mmol/L $H_2O_2$, then decreased ($P < 0.05$) at 30 mmol/L of $H_2O_2$, which may be due to the further reactions accompanied at high concentrations of $H_2O_2$ resulting in the degradation of MDA (Cao et al., 2020). It is well-established that the interaction of MDA with other compounds (e.g., proteins, phospholipids, or amino acids) could prevent their reaction with TBA (Maqsood et al., 2015). In addition, the conversion of aldehydes into other oxidation or volatile compounds by ROS could also reduce TBARs content (Serra et al., 2014). In comparison, the TBARs content in TF was relatively high, suggesting an effective enhancement of lipid oxidation ($P < 0.05$) by thermal extraction. Lipid oxidation is generally unsaturated FAs oxidation, which has been identified as a major pathway of the lipid damage in foods (Coombs et al., 2018). As a consequence, thermal extraction contributed to the decrease of the intact lipid molecules in TF samples, especially intact unsaturated lipids. Similar findings were reported by Abdulkadir and Jimoh (2013). By contrast with 0 mmol/L $H_2O_2$, the TBARs values for RF and TF samples increased by 0.022 (84.62 %) and 0.019 (47.50 %) mg MDA/kg ($P < 0.05$) in 10 mmol/L $H_2O_2$, respectively. It indicated that the lipid oxidation in RF samples occurred much faster than that in TF samples. Tu et al. (2022) reported that the high concentration of polyunsaturated FAs in tissues generally made the lipids more susceptible to oxidation (easier than monounsaturated and saturated FAs) when exposed to free radicals. The oxidation resulted in multiple changes in the target lipids, such as lipid decomposition, backbone cleavage, side-chain modifications, lipolysis, and/or composition alternations (Tu et al., 2022; Wang et al., 2024). According to Amaral et al. (2018) and Shin et al. (2019), the degree and rate of lipid oxidation highly related to the unsaturated compositions and structures of the lipid species.

### 3.4. Lipidomic profiles

#### 3.4.1. Lipid composition

The detected target lipids in the fat samples were classified and shown in Fig. 2. A total of 1168 lipid molecules was identified in RF and TF samples assigned to 18 lipid classes, of which 678 lipid species were in positive mode (Fig. 2A) and 490 lipid species were in negative mode (Fig. 2B). Among these detected lipids (Fig. 2C), 302 (25.86 %) of phosphatidylcholines (PCs), 197 (16.87 %) of phosphatidylethanolamines (PEs), 115 (9.85 %) of TGs, 92 (7.88 %) of sphingomyelins (SMs), 82 (7.02 %) of ceramides (CERs), 68 (5.82 %) of phosphatidylserines (PSs), 58 (4.97 %) of FAs, and 57 (4.88 %) of phosphatidic acids (PAs) were the major lipid classes. PC and PE, as the constituents of phospholipids, were listed as the most dominant classes of lipids. This is partly consistent with the results reported by Xiong et al. (2023) who

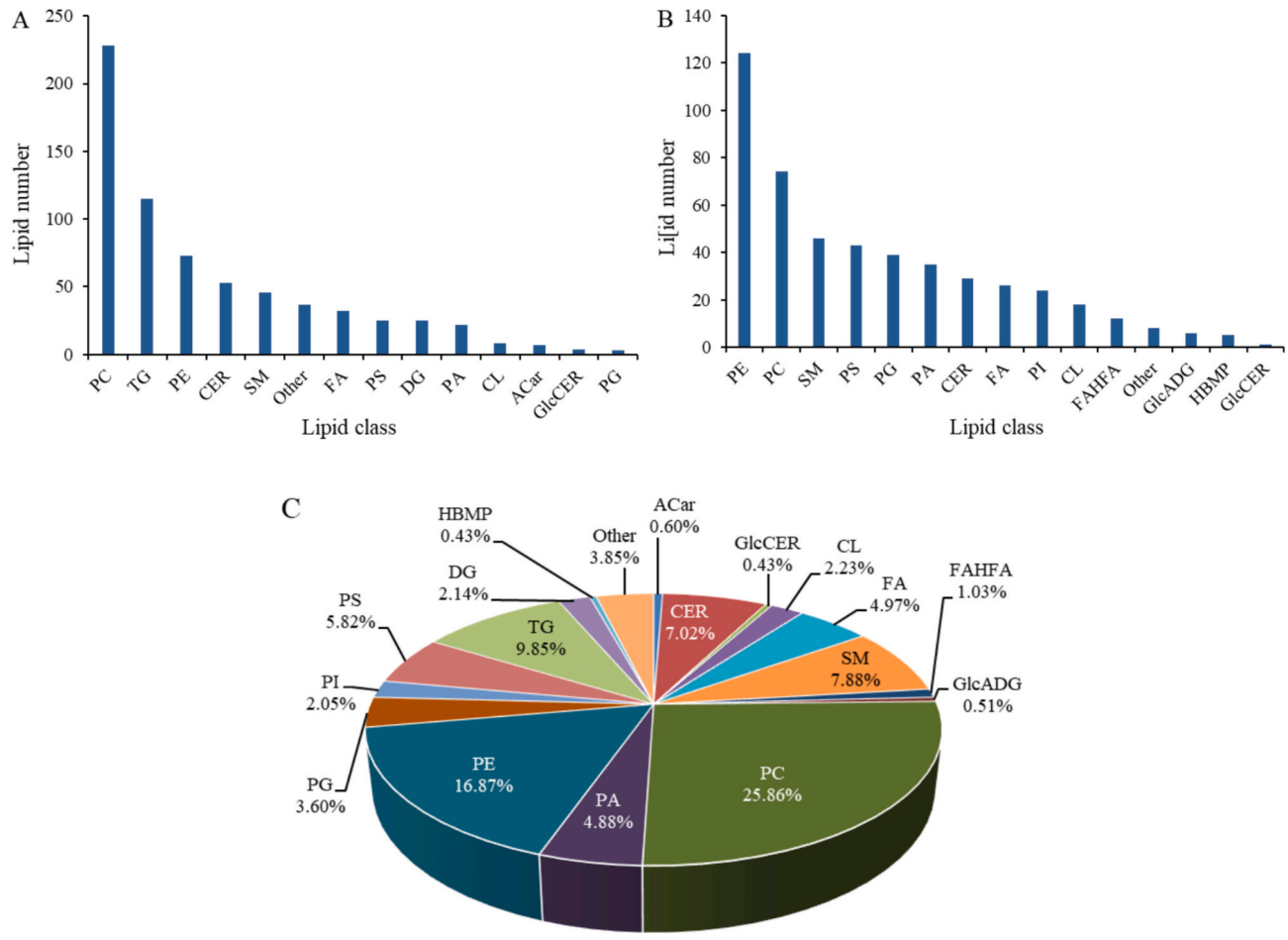


**Fig. 2.** Distribution of lipid species in ESI-positive mode (A) and ESI-negative mode (B) and lipid compositions (C) obtained from raw fat (RF) samples and thermal-extracted fat (TF) samples identified by UPLC-MS/MS analysis.

stated that PCs and TGs were the predominant lipid classes in yak subcutaneous fat. The difference in lipids was likely correlated to the breeds of yaks. It is reported that PC and PE exert important roles in the conservation of the permeability and integrity of the biological membranes, and regulation of energy, lipid metabolism, and lipoprotein secretion (Wang et al., 2024). Previous studies demonstrated that the PC and PE were closely related to the freshness, as well as the quality deterioration of animal foods (Wang et al., 2024), and were considered to be the critical lipid metabolites of animal foods during oxidation (Tu et al., 2022; Yu et al., 2020; Zhang et al., 2023). TG was the most abundant category of glycerolipids. It is confirmed that TG as an odor-inducing compound exhibits crucial roles in the flavor formation of meat products (Frank et al., 2017). These findings were coincident with the previous publications, in which the phospholipids and glycerolipids were indicated as the two main lipid classes in yak subcutaneous fat (Xiong et al., 2023) as well as in chicken abdominal fat (Li et al., 2022). Our study showed that SM was the most plentiful sphingolipids, followed by CER. SM can be converted to CER by the action of sphingomyelinase, meanwhile, it binds CER with great affinity (Goñi, 2022). Both SM and CER have profound effects on maintaining the integrity of cell membranes and regulating cell metabolism (Jia et al., 2021; Wang et al., 2024). It was documented that SMs and CERs could potentially be used to monitor the oxidative stability of lipids (Tu et al., 2022; Wang et al., 2024).

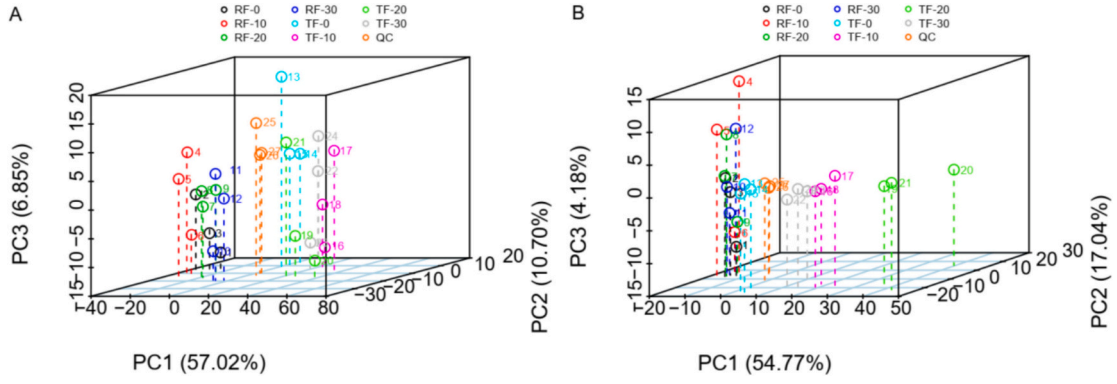


**Fig. 3.** Principal component analysis (PCA) performed on the datasets generated from UPLC-MS/MS in ESI-positive mode (A) and ESI-negative mode (B).

### 3.4.2. Overall DALs analysis

PCA score plot was used to monitor the distinction in lipidomic profiles of different treatments (Fig. 3). The result indicated that QC samples were closely clustered together in either positive or negative mode, confirming a good analytical repeatability. Moreover, clear separation was observed between RF and TF samples suggesting significant differences in their lipidome profiles.

According to VIP $\geq$1 along with FC $\geq$2 or $\leq$ 0.5 deemed as DALs, 432 (236 in positive ions and 196 in negative ions) differential lipid species was identified (shown in Supplemental Table S1). To get a further insight into the similarities of RF and TF samples during the oxidation, the heatmap combined with hierarchical clustering analysis (HCA) based on the target DALs was employed. The result (Fig. 4A and B) showed remarkable differences occurred between RF and TF samples regardless of electrospray ionization. The findings were in line with those in PCA (shown in Fig. 3). It was indicated that lipid compounds in the TF samples were significantly differed from that in the RF samples, which affirmed that the thermal extraction obviously altered the lipidomic profiles in yak fat. This might be associated with the fact that the lipids undergo a series of reactions including lipid decomposition, C—C bone breakdown, side-chain alterations, and/or lipolysis in the heating process (Zhuang et al., 2022). Furthermore, remarkable differences in the abundance of some lipids in both RF and TF samples were also noted with the increase of $H_2O_2$ concentration. The lipids in TF samples derived from various oxidative conditions were categorized into two main clusters, one cluster for TF samples treated with 0 mmol/L $H_2O_2$, and another for the samples treated with 10, 20, and 30 mmol/L $H_2O_2$. Besides, the difference between the samples treated with 20 and 30 mmol/L $H_2O_2$ was not significant, which could be classified as one small group. Lipids in RF samples treated with 0 and 30 mmol/L $H_2O_2$ shared similar profile, while those treated with 10 and 20 mmol/L $H_2O_2$ had much more similarities. To a certain extent, the HCA results were consistent with those observed in peroxide value and TBARs content.

### 3.4.3. Changes of differentially abundant phospholipids, TGs, FAs and CERs

Phospholipids can be mainly classified into PC, PE, PS, PA, phosphatidylglycerol (PG) and phosphatidylinositol (PI) according to their

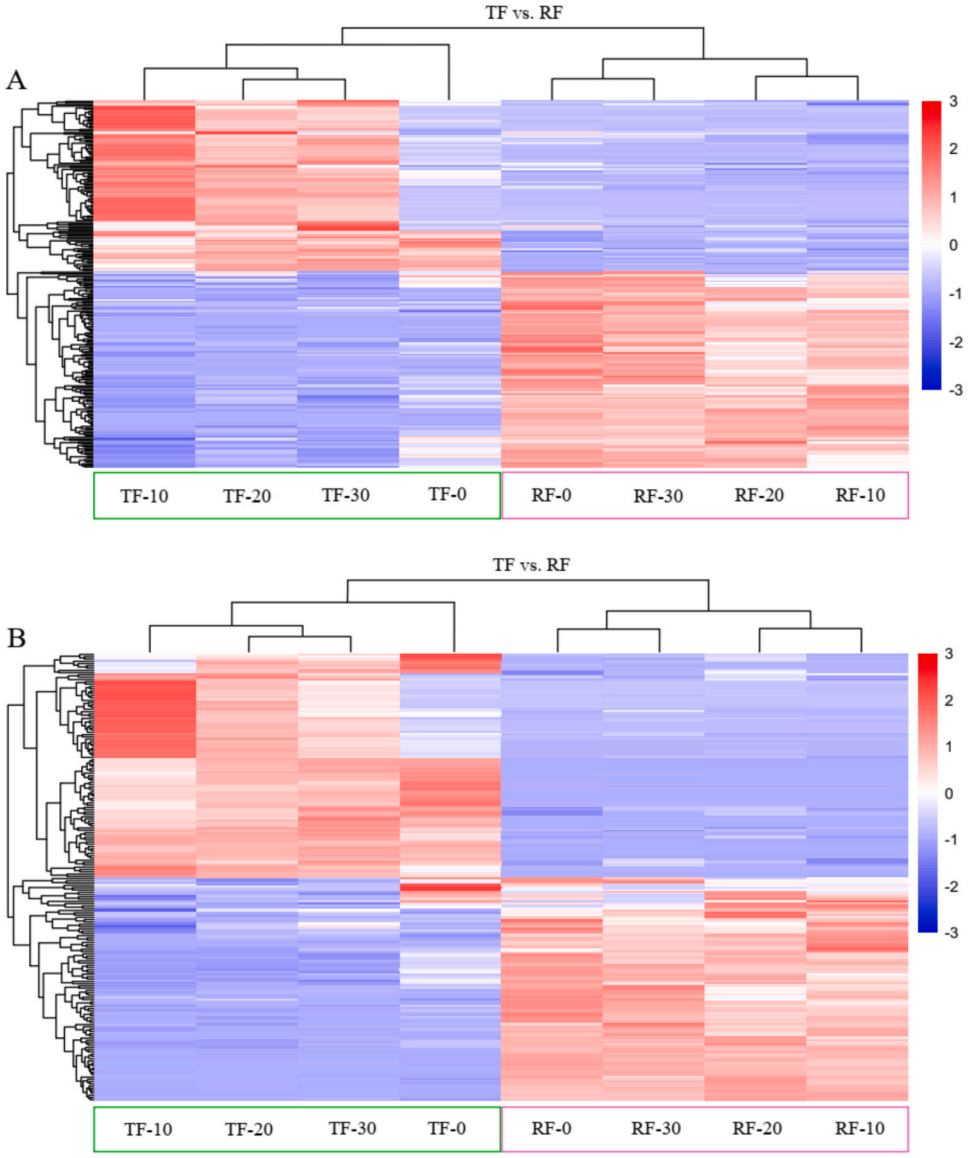


**Fig. 4.** Hierarchical clustering of differentially abundant lipids in ESI-positive mode (A) and ESI-negative mode (B). In the color scale (at right), red and blue indicate increased and decreased levels of differentially abundant lipids. (For interpretation of the references to color in this figure legend, the reader is referred to the web version of this article.)

characteristic groups (Zhang et al., 2021). In present study, a total of 276 differentially abundant phospholipids were identified in RF and TF samples, including 82 species of PCs, 66 species of PEs, 57 species of PSs, 42 species of PAs, 20 species of PGs, and 9 species of PIs. Several studies revealed that high temperature, active radicals, and/or strong light caused oxidative damage to phospholipid (Song et al., 2020; Tu et al., 2022; Zhang et al., 2023). The oxidation of phospholipids usually occurred at unsaturated bonds to form phospholipid hydroperoxide, which is unstable and cleaved into long-chain and short-chain oxidation products, affecting the flavor and nutritional quality of animal foods (Zhang et al., 2023).

The effects of thermal extraction and oxidative stress on phospholipids are shown in Fig. 5 (A-F). Statistical analysis suggested that $H_2O_2$ treatment and fat type had influential effects on the PC, PE, PS, PA, PG or PI value ($P < 0.05$), and their interaction had a remarkable effect on the PS, PG, PA or PI content ($P < 0.05$). As illustrated in Fig. 5A, there were relatively lower contents of PC in TF samples comparing to RF samples ($P < 0.05$). In light of the report of Li et al. (2020), thermal treatment contributed to the remarkable reduction of the polar molecules of PC in the muscle tissues, which was in harmony with our results. The decrease in abundance of PC might be attributed to the cleavage of C—C species of the $\alpha$-bond close to the functional groups and hydrogen rearrangements (Liu et al., 2018). PCs in RF samples showed a decrease at 10 mmol/L $H_2O_2$ ($P < 0.05$), then remained at stable values from 10 to 30 mmol/L $H_2O_2$, while the values in TF samples decreased ($P < 0.05$) at first, followed by an increment ($P < 0.05$). Tu et al. (2022) observed significant decreases in PC contents in oxidized shrimp treated with 4 mmol/L $H_2O_2$ by contrast with that in fresh shrimp. However, the increase in PC contents in TF samples might be related to the event that high concentrations of free radicals combined with thermal extraction damaged the cell membrane, resulting in the release of PCs. After all, cell membranes are more sensitive to free radicals after heating. In Fig. 5B, the PE values in TF samples were remarkably lower than that in RF samples ($P < 0.05$). Similar decreases in PE contents were observed in the lipid extracts (Zhou et al., 2019). The PE levels in both RF and TF samples decreased ($P < 0.05$) at 10 mmol/L $H_2O_2$ and maintained steady ($P > 0.05$) from 10 to 20 mmol/L $H_2O_2$, subsequently increased ($P < 0.05$) at 30 mmol/L $H_2O_2$. It was observed that the lower contents of PE were closely related to the higher values of peroxide and TBARs detected in the samples. Wang et al. (2024) also reported that lipid oxidation was probably responsible for the changes in PE content, and PE content was negatively correlated with TBARs and peroxide values. The detected PSs (Fig. 5C) and PGs (Fig. 5D) significantly reduced in the TF samples, compared with the RF samples. The leading cause responsible for the loss of PGs was the oxidation that took place during heating (Zhang et al., 2023). Regardless of fat matrix, along with the rising of $H_2O_2$ concentrations, the contents of PS declined ($P < 0.05$), then remained steady ($P > 0.05$). However, the PGs showed a down-upward trend as $H_2O_2$ concentration increased from 0 to 30 mmol/L. Amazingly, the relative abundance of PA in RF samples was found to be higher ($P < 0.05$) than TF samples (Fig. 5E). This inferred that these PAs were resistant to thermal extraction, as shown by the oxidation rate of PAs

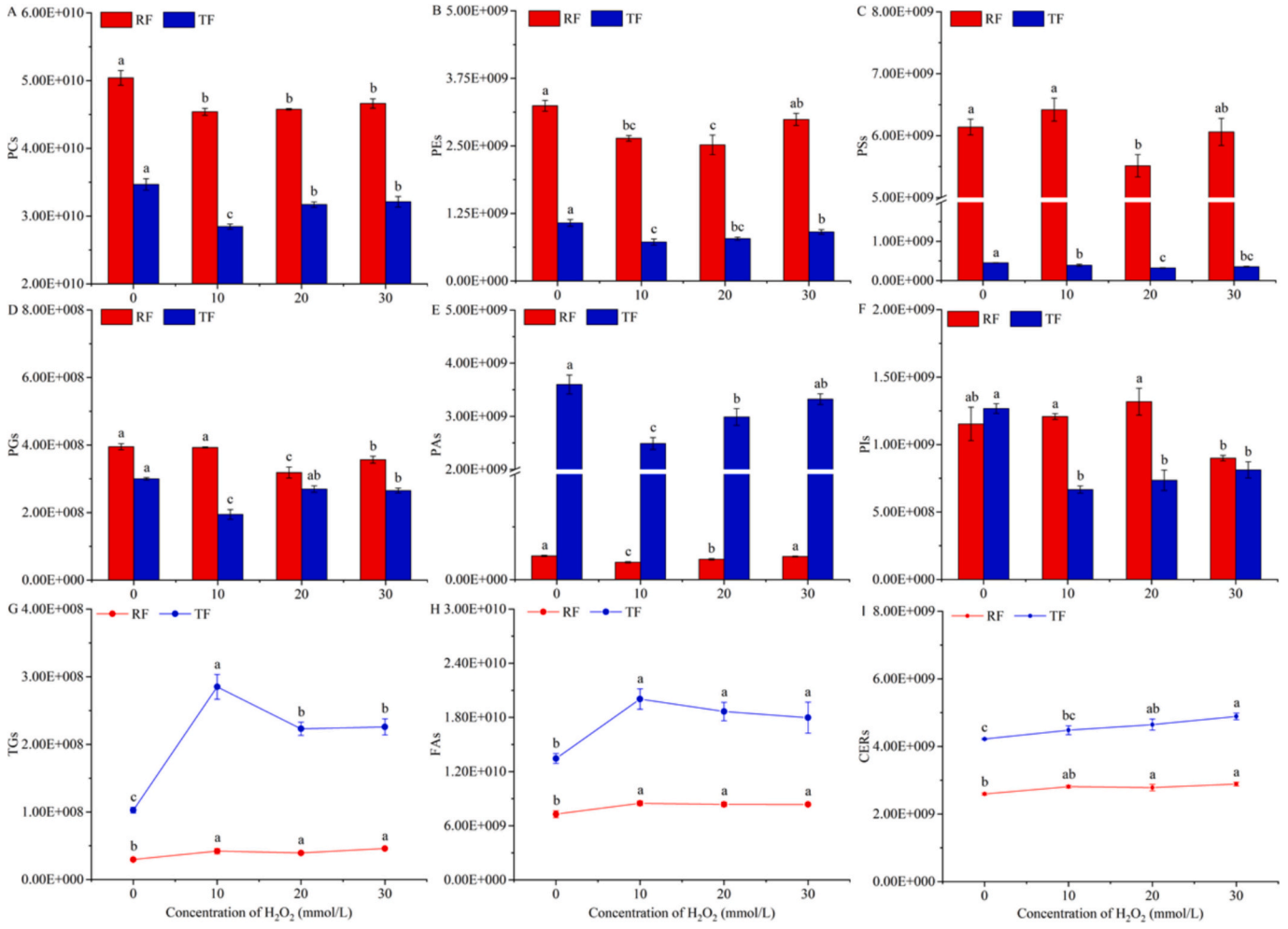


**Fig. 5.** Changes in the total PC (A), PE (B), PS (C), PG (D), PA (E), PI (F), TG (G), FA (H), and CER (I) contents in raw fat (RF) samples and thermal-extracted fat (TF) samples. Error bars represent the standard error. [a-c]Means with different lowercase letters are significantly different among $H_2O_2$ treatments ($P < 0.05$).

being lower than theirs release rate. The changes in PA contents showed a similar trend with that in PG. The RF and TF samples treated with 0 or 30 mmol/L $H_2O_2$ displayed similar PI contents ($P > 0.05$, Fig. 5F), while the RF treated with 10 or 20 mmol/L $H_2O_2$ had higher PI values compared to TF samples ($P < 0.05$). It was not difficult to find that thermal extraction had little effect on PI contents compared with the above phospholipids. The PI values in RF samples increased ($P > 0.05$) slightly at 20 mmol/L $H_2O_2$ and then decreased ($P < 0.05$) significantly at 30 mmol/L $H_2O_2$. Whereas, the PI values in TF samples decreased ($P < 0.05$) at 10 mmol/L $H_2O_2$ followed by a stable phase ($P > 0.05$) from 10 to 30 mmol/L $H_2O_2$. Wang et al. (2024) reported that PI constructed with long unsaturated fatty acyl chains was more tolerant of oxidative degradation, which is in accordance with our observations.

TG consists of one glycerol and three fatty acids, and its function is determined by the type of fatty acids. Remarkable increases in TGs including TG(18:1(9Z)/18:1(9Z)/18:2(9Z,12Z)) [iso3], TG(16:1(9Z)/18:1(9Z)/18:1(9Z)) [iso3], TG(16:1(9Z)/16:1(9Z)/20:4(5Z,8Z,11Z,14Z)) [iso3], TG(18:2(9Z,12Z)/20:1(11Z) /20:1(11Z)) [iso3], and TG(16:0/16:1(9Z)/16:1(9Z)) [iso3] were identified after thermal extraction (Fig. 5G), it suggested the cell membrane of adipose tissue was destructed during the heating, and consequently TGs released into the samples were higher than the oxidation or hydrolysis of TGs. Zhou et al. (2023) disclosed that the TGs contents in crayfish meat exhibited an upward trend after various thermal processing treatments. Upon •OH oxidation, the relative contents of TG in RF samples increased ($P < 0.05$) although there was no significant difference among various $H_2O_2$ treatments, and the TG values in TF samples increased to the largest values ($P < 0.05$) at 10 mmol/L $H_2O_2$, subsequently declined. These results were partially consistent with the previous study reported by Tu et al. (2022), in which the main TGs increased obviously in oxidized samples exposed to a hydroxyl-radical-generating system. The reduction in TG might be owing to the dominance of oxidative degradation under high dosage of free radical (Da Silva et al., 2006). Generally, $H_2O_2$ concentration, fat type, and their interaction significantly affected the TG content ($P < 0.05$).

FAs can be divided into short-chain (< 6 carbon), medium-chain (6–12 carbon), long-chain (13–21 carbon) and very long-chain (> 22 carbon) FAs. It was well documented that the FAs were closely correlated with the organoleptic quality of meat and meat products (Wang et al., 2024). As illustrated in Fig. 5H, $H_2O_2$ concentration, fat type, or their interaction showed an observable effect on the FA content ($P < 0.05$). The contents of differentially abundant FAs, such as oleic acid, sterculic acid, myristoleic acid, margaric acid, heptadecanedioic acid and docosatrienoic acid, etc., increased significantly ($P < 0.05$) after thermal extraction or incubation in oxidizing agent indicating that the oxidation/degradation of phospholipids and TGs was more likely to occur than the oxidation of FAs in this study. These released FAs are readily oxidized to form various primary oxidative products such as epoxy, hydroxyl, and hydroperoxy FAs (Zhang et al., 2021).

CERs are essential intermediates in the biosynthesis of all complex sphingolipids, and produced by coupling long-chain FAs onto the backbone sphingoid bases by amide binds, which possibly serve as signaling molecules to regulate various cellular metabolic pathway such as cell proliferation and apoptosis as well as stress response (Jia et al., 2021). As shown in Fig. 5I, it was observed that both thermal extraction and $H_2O_2$ concentration significantly raised ($P < 0.05$) CER contents. C2-ceramide, Cer-NS (d16:1/16:0), Cer-NS (d16:1/24:0), Ceramide 5, C24 Phytoceramide (t18:0/24:0), Glucosylceramide (d18:1/18:0), Cer-NDS (d17:0/16:0), and C16 1-Deoxyceramide (m18:1/16:0) represented the major CERs. As reported by Andrieu-Abadie et al. (2001), oxidative stress has been known to promote CERs generation. The increase in CERs could be due to the lipid transformations triggered by the attack of ROS (Wang et al., 2024). However, the interaction of $H_2O_2$ concentration and fat treatment did not obviously affect the CER contents ($P > 0.05$).

## 4. Conclusion

In this study, the lipid oxidation and lipidomic profiles of RF and TF samples under hydroxyl radical-induced oxidative stress were investigated. Chemical analysis results suggested that both thermal extraction and hydroxyl radicals noticeably exacerbated yak lipid oxidation. The PCA suggested that significant alterations in lipidomic profiles were observed between RF and TF, and the comparative lipidomics analysis further indicated that 432 DALs were identified in the RF and TF samples after treated with the hydroxyl-radical-generating system. The RF samples exhibited a higher proportion of PCs, PEs, PSs, PGs, and PIs, whereas the TF samples displayed a higher abundance of PAs, TGs, FAs, and CERs among lipid species. This study provides new insights into the comprehension of the alterations in lipid profiles induced by thermal extraction and hydroxyl radical attack in yak fat. The impacts of hydroxyl radical oxidation combined with thermal processing on lipid decomposition are very complicated, current research data are still insufficient to disclose the mechanism of the lipid degradation, and more research are required concerning the thermal extraction related to lipid oxidation, particularly the lipid metabolic pathway, intermediate and final products.

## CRediT authorship contribution statement

**Sining Li:** Writing – review & editing, Writing – original draft, Supervision, Methodology, Investigation. **Shanhu Tang:** Writing – review & editing, Project administration, Funding acquisition, Conceptualization. **Ran Mo:** Software, Methodology, Data curation, Conceptualization. **Pinglian Yu:** Software, Methodology.

## Declaration of competing interest

The authors declare that they have no known competing financial interests or personal relationships that could have appeared to influence the work reported in this paper.

## Acknowledgements

This work was financially supported by the Sichuan Provincial Science and Technology Program (No. 2024YFTX0010; 2022ZHCG0129).

## Appendix A. Supplementary data

Supplementary data to this article can be found online at https://doi.org/10.1016/j.fochx.2025.102295.

## Data availability

Data will be made available on request.

## References

Abdulkadir, A. G., & Jimoh, W. L. O. (2013). Comparative analysis of physico-chemical properties of extracted and collected palm oil and tallow. *ChemSearch Journal, 4*(2), 44–54.

Abeyrathne, E. D. N. S., Nam, K., & Ahn, D. U. (2021). Analytical methods for lipid oxidation and antioxidant capacity in food systems. *Antioxidants, 10*(10), 1587. https://doi.org/10.3390/antiox10101587

Amaral, A. B., da Silva, M. V., & da Silva Lannes, S. C. (2018). Lipid oxidation in meat: Mechanisms and protective factors - a review. *Food Science and Technology, 38*(29), 1–15. https://doi.org/10.1590/fst.32518

Andrieu-Abadie, N., Gouaźe, V., Salvayre, R., & Levade, T. (2001). Ceramide in apoptosis signaling: Relationship with oxidative stress. *Free Radical Biology and Medicine, 31*, 717–728. https://doi.org/10.1016/S0891-5849(01)00655-4

Bao, Y. F., & Pignitter, M. (2023). Mechanisms of lipid oxidation in water-in-oil emulsions and oxidomics-guided discovery of targeted protective approaches. *Comprehensive Reviews in Food Science and Food Safety, 22*(4), 2678–2705. https://doi.org/10.1111/1541-4337.13158

Beavers, W. N., Serwa, R., Shimozu, Y., Tallman, K. A., Vaught, M., Dalvie, E. D., … Potter, N. A. (2014). ω-Alkynyl lipid surrogates for polyunsaturated fatty acids: Free

radical and enzymatic oxidations. *Journal of the American Chemical Society, 136*(32), 11529–11539. https://doi.org/10.1021/ja506038v

Boran, G., Karacam, H., & Boran, M. (2006). Changes in the quality of fish oils due to storage temperature and time. *Food Chemistry, 98*(4), 693–698. https://doi.org/10.1016/j.foodchem.2005.06.041

Cao, Y. G., Ma, W. H., Wang, J. H., Zhang, S. H., Wang, Z. Y., Zhao, J., … Zhang, D. Q. (2020). Influence of sodium pyrophosphate on the physicochemical and gelling properties of myofibrillar protein under hydroxyl radical-induced oxidative stress. *Food & Function, 11*(3), 1996–2004. https://doi.org/10.1039/C9FO02412C

China. (2018). *S.A.C. China Operating procedure of livestock and poultry slaughtering-Cattle (GB/T 19477–2018) Standards Press of China*. Beijing. *2018*.

Coombs, C. E. O., Holman, B. W. B., Ponnampalam, E. N., Morris, S., Friend, M. A., & Hopkins, D. L. (2018). Effects of chilled and frozen storage conditions on the lamb *M. longissimus lumborum* fatty acid and lipid oxidation parameters. *Meat Science, 138*, 116–122. https://doi.org/10.1016/j.meatsci.2017.10.013

Da Silva, M. A., Sanches, C., & Amante, E. R. (2006). Prevention of hydrolytic rancidity in rice bran. *Journal of Food Engineering, 75*, 487–491. https://doi.org/10.1016/j.jfoodeng.2005.03.066

Frank, D., Kaczmarska, K., Paterson, J., Piyasiri, U., & Warner, R. (2017). Effect of marbling on volatile generation, oral breakdown and in mouth flavor release of grilled beef. *Meat Science, 133*, 61–68. https://doi.org/10.1016/j.meatsci.2017.06.006

Goñi, F. M. (2022). Sphingomyelin: What is it good for? *Biochemical and Biophysical Research Communications, 633*, 23–25. https://doi.org/10.1016/j.bbrc.2022.08.074

Jia, W., Li, R. T., Wu, X. X., Liu, L., Liu, S. X., & Shi, L. (2021). Molecular mechanism of lipid transformation in cold chain storage of tan sheep. *Food Chemistry, 347*, Article 129007. https://doi.org/10.1016/j.foodchem.2021.129007

Jongberg, S., Skov, S. H., Tørngren, M. A., Skibsted, L. H., & Lund, M. N. (2011). Effect of white grape extract and modified atmosphere packaging on lipid and protein oxidation in chill stored beef patties. *Meat Science, 128*(2), 276–283. https://doi.org/10.1016/j.foodchem.2011.03.015

Kanner, J. (1994). Oxidative processes in meat and meat products: Quality implications. *Meat Science, 36*(1–2), 169–189. https://doi.org/10.1016/0309-1740(94)90040-x

Li, C., Li, X. F., Huang, Q. L., Zhuo, Y., Xu, B. C., & Wang, Z. P. (2020). Changes in the phospholipid molecular species in water-boiled salted duck during processing based on shotgun lipidomics. *Food Research International, 132*, 109064. https://doi.org/10.1016/j.foodres.2020.109064

Li, J., Zhang, J. Q., Yang, Y. Y., Zhu, J. W., He, W. Z., Zhao, Q. Y., … Zhang, J. M. (2021). Comparative characterization of lipids and volatile compounds of Beijing Heiliu and Laiwu Chinese black pork as markers. *Food Research International, 146*, Article 110433. https://doi.org/10.1016/j.foodres.2021.110433

Li, J. J., Li, Z. Q., Ran, J. S., Yang, C. W., Lin, Z. Z., & Liu, Y. P. (2022). LC/MS-based lipidomics to characterize breed-specific and tissue-specific lipid composition of chicken meat and abdominal fat. *LWT- Food Science and Technology, 163*, Article 113611. https://doi.org/10.1016/j.lwt.2022.113611

Liu, Y. Z., Cong, P. X., Li, B. J., Song, Y., Liu, Y. J., Xu, J., & Xue, C. H. (2018). Effect of thermal processing towards lipid oxidation and non-enzymatic browning reactions of Antarctic krill (*Euphausia superba*) meal. *Journal of the Science of Food and Agriculture, 98*(14), 5257–5268. https://doi.org/10.1002/jsfa.9064

Maqsood, S., Abushelaibi, A., Manheem, K., Rashedi, A. A., & Kadim, I. T. (2015). Lipid oxidation, protein degradation, microbial and sensorial quality of camel meat as influenced by polyphenolic compounds. *LWT- Food Science and Technology, 63*(2), 953–959. https://doi.org/10.1016/j.lwt.2015.03.106

Nam, K. H. (2022). Beef tallow injection matrix for serial crystallography. *Scientific Reports, 12*(1), 694. https://doi.org/10.1038/s41598-021-04714-6

Serra, A., Buccioni, A., Rodriguez-Estrada, M. T., Conte, G., Cappucci, A., & Mele, M. (2014). Fatty acid composition, oxidation status and volatile organic compounds in "Colonnata" lard from large white or Cinta Senese pigs as affected by curing time. *Meat Science, 97*(4), 504–512. https://doi.org/10.1016/j.meatsci.2014.03.002

Shantha, N. C., & Decker, E. A. (1994). Rapid, sensitive, iron-based spectrophotometric methods for determination of peroxide values of food lipids. *Journal of AOAC International, 77*(2), 421–424. https://doi.org/10.1093/jaoac/77.2.421

Shin, D. M., Kim, D. H., Yune, J. H., Kwon, H. C., Kim, H. J., Seo, H. G., & Han, S. G. (2019). Oxidative stability and quality characteristics of duck, chicken, swine and bovine skin fats extracted by pressurized hot water extraction. *Food Science of Animal Resources, 39*(3), 446–458. https://doi.org/10.5851/kosfa.2019.e41

Song, G. S., Li, L. Q., Wang, H. X., Zhang, M. N., Yu, X. N., Wang, J., … Shen, Q. (2020). Real-time assessing the lipid oxidation of prawn (*Litopenaeus vannamei*) during air-frying by iKnife coupling rapid evaporative ionization mass spectrometry. *Food Control, 111*, Article 107066. https://doi.org/10.1016/j.foodcont.2019.107066

Song, S. Q., Zhang, X. M., Hayat, H., Liu, P., Jia, C. S., Xia, S. Q., … Niu, Y. W. (2011). Formation of the beef flavour precursors and their correlation with chemical parameters during the controlled thermal oxidation of tallow. *Food Chemistry, 124*(1), 203–209. https://doi.org/10.1016/j.foodchem.2010.06.010

Tu, C. H., Qi, X. E., Shui, S. S., Lin, H. M., Benjakul, S., & Zhang, B. (2022). Investigation of the changes in lipid profiles induced by hydroxyl radicals in whiteleg shrimp (*Litopenaeus vannamei*) muscle using LC/MS-based lipidomics analysis. *Food Chemistry, 369*, Article 130925. https://doi.org/10.1016/j.foodchem.2021.130925

Wang, L., Zang, M. W., Cheng, X. Y., Wang, S. W., Zhao, X., Zhao, B., & Li, D. (2024). Evaluation of changes in the lipid profiles of dried shrimps (*Penaeus vannamei*) during accelerated storage based on chemical and lipidomics analysis. *LWT- Food Science and Technology, 191*, Article 115564. https://doi.org/10.1016/j.lwt.2023.115564

Wojtasik-Kalinowska, I., Górska-Horczyczak, E., Stelmasiak, A., Marcinkowska-Lesiak, M., Onopiuk, A., Wierzbicka, A., & Półtorak, A. (2021). Effect of temperature and oxygen dose during rendering of goose fat to promote fatty acid profiles. *European Journal of Lipid Science and Technology, 123*, Article 2100085. https://doi.org/10.1002/ejlt.202100085

Xiong, L., Pei, J., Bao, P. J., Wang, X. D., Guo, S. K., Cao, M. L., … Guo, X. (2023). The effect of the feeding system on fat deposition in yak subcutaneous fat. *International Journal of Molecular Sciences, 24*, 7381. https://doi.org/10.3390/ijms24087381

Xiong, L., Pei, J., Wu, X. Y., Bao, P. J., Guo, X., & Yan, P. (2022). Explaining unsaturated fatty acids (UFAs), especially polyunsaturated fatty acid (PUFA) content in subcutaneous fat of yaks of different sex by differential proteome analysis. *Genes, 13*, 790. https://doi.org/10.3390/genes13050790

Yu, M. M., Gang, K. Q., Li, C., Wang, J. H., Liu, Y. X., Zhou, D. Y., & Zhu, B. W. (2020). Change of lipids in whelks (*Neptunea arthritica cumingi* Crosse and *Neverita didyma*) during cold storage. *Food Research International, 136*, Article 109330. https://doi.org/10.1016/j.foodres.2020.109330

Zeb, A., & Akbar, A. (2018). Ellagic acid suppresses the oxidative stress induced by dietary-oxidized tallow. *Oxidative Medicine and Cellular Longevity, 2018*, Article 7408370. https://doi.org/10.1155/2018/7408370

Zhang, D., Li, X. J., Duan, X. L., Sun, H., & Cao, Y. P. (2021). Lipidomics reveals the changes in lipid profile of flaxseed oil affected by roasting. *Food Chemistry, 364*, Article 130431. https://doi.org/10.1016/j.foodchem.2021.130431

Zhang, L. T., Shan, Y. K., Hong, H., Luo, Y. K., Hong, X. H., & Ye, W. J. (2020). Prevention of protein and lipid oxidation in freeze-thawed bighead carp (*Hypophthalmichthys nobilis*) fillets using silver carp (*Hypophthalmichthys molitrix*) fin hydrolysates. *LWT-Food Science and Technology, 123*, Article 109050. https://doi.org/10.1016/j.lwt.2020.109050

Zhang, M. H., Xie, D. N., Wang, D. Y., Xu, W. M., Zhang, C. H., Li, P. P., & Sun, C. (2023). Lipidomic profile changes of yellow-feathered chicken meat during thermal processing based on UPLC-ESI-MS approach. *Food Chemistry, 399*, Article 133977. https://doi.org/10.1016/j.foodchem.2022.133977

Zhou, M. Z., Liu, D. Y., Qiu, W. X., Wang, C., Yu, W., Xiong, G. Q., … Qiao, Y. (2023). Lipidomics and GC-MS analyses of key lipids for volatile compound formation in crayfish meat under different thermal processing treatments. *LWT- Food Science and Technology, 189*, Article 115522. https://doi.org/10.1016/j.lwt.2023.115522

Zhou, X., Zhou, D. Y., Liu, Z. Y., Yin, F. W., Liu, Z. Q., Li, D. Y., & Shahidi, F. (2019). Hydrolysis and oxidation of lipids in mussel *Mytilus edulis* during cold storage. *Food Chemistry, 272*, 109–116. https://doi.org/10.1016/j.foodchem.2018.08.019

Zhu, J. F., Lin, W. F., Sun, Y. Y., Pan, D. D., Xia, Q., Zhou, C. Y., & He, J. (2024). Relationship between flavor characteristics and lipid oxidation in air-dried beef at different roasting stages. *International Journal of Gastronomy and Food Science, 37*, Article 100988. https://doi.org/10.1016/j.ijgfs.2024.100988

Zhuang, Y., Dong, J., He, X. M., Wang, J. P., Li, C. M., Dong, L., … Wang, S. (2022). Impact of heating temperature and fatty acid type on the formation of lipid oxidation products during thermal processing. *Frontiers in Nutrition, 9*, Article 913297. https://doi.org/10.3389/fnut.2022.913297